

Patterning by a morphogen gradient and lateral inhibition.

Author: Robert Cañellas Núñez.

*Facultat de Física, Universitat de Barcelona, Diagonal 645, 08028 Barcelona, Spain.**

Advisor: Marta Ibañez

(Dated: January 16, 2018)

Abstract: Patterns emerge in a wide range of systems that initially were homogeneous. We focused on a model of a developing tissue that responds to two types of signals that correspond to two distinct spatial communications, a long-range communication set by a morphogen gradient and interactions between adjacent cells mediated by two transmembrane proteins. Analysing the accessible steady states we saw, for intermediate signals, bistable responses of cells. When cells interact between them, lateral inhibition appears and a fine-grained pattern with a period 2 emerges. Simulating the dynamics we explored different initial conditions and the results agree with the linear stability analysis.

I. INTRODUCTION

In developing embryonic tissues, cells that initially are equivalent become different creating patterns [1][2]. This process can involve different strategies to reach a spatial pattern of distinct cell types [3]. For instance, it can involve different types of spatial communication and here we study two of them: (i) long-range communication through a morphogen gradient [4] and (ii) short-range communication by cell-cell interactions [5]. Both of them are present in the fruit fly (*Drosophila melanogaster*), one of the most studied organisms by its easy geometry and simplicity compared to other biological systems [6].

During embryonic development some cells within tissues can secrete proteins that can form an extracellular gradient across the whole tissue through diffusion, for instance. The secreted protein acts as a morphogen when it activates target genes in a concentration-dependent manner in other cells. These cells sense the extracellular protein concentration, transduce it to the nucleus and give different responses according to it [4]. So this mechanism can provide positional information to cells and drive them to specific fates that depend on the extracellular concentration. This type of long range positional information sets the body plan of *Drosophila* [7].

One way of short-range communication between cells is through two types of transmembrane proteins, ligands and receptors, that are anchored in the cell membrane. It is assumed that each cell has the ligand and receptor, can signal and respond to signals. When a ligand binds to a receptor in an adjacent cell they trigger a reaction that activates a gene expression, change the metabolism of the cell or another type of cell response like initiation of cell differentiation within the cell that harbors the receptor [2],[5].

Recently, *Corson* et al have seen these types of spatial communication driving cell fate-specification. In the tissue studied by them [8], the notum of *Drosophila* during pupal development, cells differentiate into two types of fates, sensory organ precursor (SOP) and epidermal. The results indicate that without any signal the cell fate adopted corresponds to SOP but, if cells receive a signal, an inhibition takes place and the epidermal fate is adopted. As we said, the signal can come from both types of spatial communication but when the signal is emitted by the neighboring cells the phenomenon is known as lateral inhibition.

II. THE MODEL

We used a mathematical approach of Notch signaling and fate-specification formulated by *Corson* et al [8], which considers both morphogen gradients and cell-cell communication. The model studied here is a simplified deterministic version of that analysed by *Corson* et al [8]. Cell state dynamics is described by a nonlinear differential equation with only one variable, u_i , that describes the state of the cell i having values between 0 and 1. For low values of u the state corresponds to low proneural activity or epidermal fate, and for high values to high proneural activity or SOP. The dynamics of cell state depends on signals, s , that the cell receives and which inhibit the SOP fate. When we studied the dynamics with a morphogenic gradient (case i), the signal received by the cell i was the concentration of the ligand at the position i , c_i . When we only had cell-cell communication (case ii) we used a linear dependence between the signal and the states of the nearest-neighbors. These nearest-neighbors, (nn), of cell i were only those that were in contact, because as we said ligands and receptor are anchored at the membrane, thus they have to be in contact to bind.

So for each case:

*Electronic address: robertcanye@gmail.com

i.

$$s = c_i \quad (1)$$

ii.

$$s = \sum_{j \in nn} u_j \quad (2)$$

As we said the dynamics of the state of a cell is governed by the following differential equation and can be related to gene regulation [8]:

$$\frac{du}{dt} = f(u - s) - u = g(u, s) \quad (3)$$

Corson et al. [8] use a sigmoid function for f because it is monotonic, increasing for u and decreasing for s , according with the amplification of SOP fate by u and inhibition of SOP fate by s . The sigmoid function used is as proposed in [8]:

$$f(u - s) = \frac{1 + \tanh(4(u - s))}{2} \quad (4)$$

III. METHODS AND RESULTS.

A. Steady states driven by a gradient.

1. Bifurcation diagram and linear stability analysis.

The steady states, u_0 , that a cell can reach receiving a constant signal s are obtained when the dynamics reach the stationary regime, $\frac{du}{dt} = 0$. Steady states (Fig. 1a) correspond to the intersections of f and u .

We explored the steady states for signals of values between 0 and 1 and used the Newton Raphson algorithm [10], beginning with $s = 0$ and using a step of $ds = 10^{-3}$. The bifurcation diagram (Fig. 1b) obtained is consistent with the results of Corson et al [8]. If s is very low (there is no inhibitory signal (or nearly)) the cell adopts the SOP fate, while if s is high the cell adopts the epidermal fate. It is when the signal is intermediate that the results indicate that there are three stationary states, one with intermediate cell state values. However, we will show this one is unstable.

To study the stability of these states, we took a small perturbation around all steady states, $u_i = u_0 + w_i$, and linearize the equation of dynamics. Our resulting equation is a normal eigenvalue ODE:

$$\frac{dw}{dt} = \lambda w \quad (5)$$

with $\lambda = \frac{dg}{du} \Big|_{u_0}$

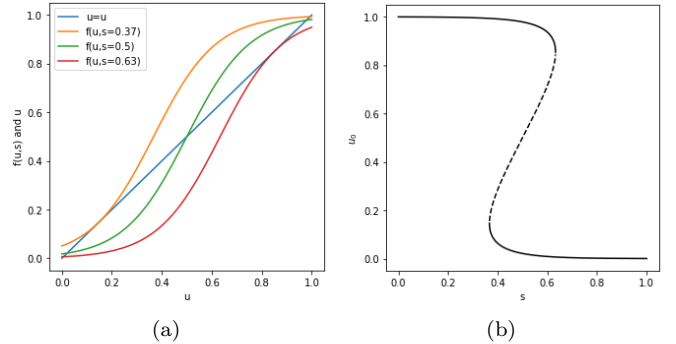


FIG. 1: (a) Intersection of the function $f(u - s)$ and u , using different values of s . (b) Bifurcation diagram with stable (continuous) and unstable (dashed) steady states.

If $\lambda < 0$ (notice it is Real) the initial perturbation will decrease over time and vanish, hence the state u_0 is linearly stable. But if $\lambda > 0$, the initial perturbation will grow over time and the state is unstable. The results of the analysis indicate that at intermediate values of the signal the cell states corresponding to SOP and epidermal fates are stable, whereas the intermediate cell state is unstable (Fig. 1b).

2. Numerical integration of the dynamics.

To prove our results of the steady states we simulated the dynamics for a square array of cells with periodic boundary conditions, using a Euler or Runge-Kutta fourth-order method, [10]. As the RK4 performed more time than the first one and did not show an improvement we finally only used Euler with a step of time $dt = 0.01$, beginning at $t = 0$ and integrating up to $t = 100$.

To analyse the response within a range of s constant values, we considered a gradient of s values across the tissue of $N \times N$ cells. The gradient of the signal that we imposed had the form:

$$s(x_i) = c_i = \begin{cases} 1 - \frac{x_i}{N}, & x_i > 0 \\ 1 + \frac{x_i}{N}, & x_i < 0 \end{cases} \quad (6)$$

This variable x_i corresponds to the position of the cell i along the x axis. For a linear array of cells, the origin is centered to have symmetry over the y axis. It can be seen that at $x = 0$ cells receive a maximum signal and, the signal decreases linearly, reaching the minimum at the furthest cells (Fig. 2). Yet, we could simulate only a linear array of cells because the gradient is only over the x axis. We decided to use a square array of cells because at the end, we will study the whole model with both types of spatial communications and we will see some

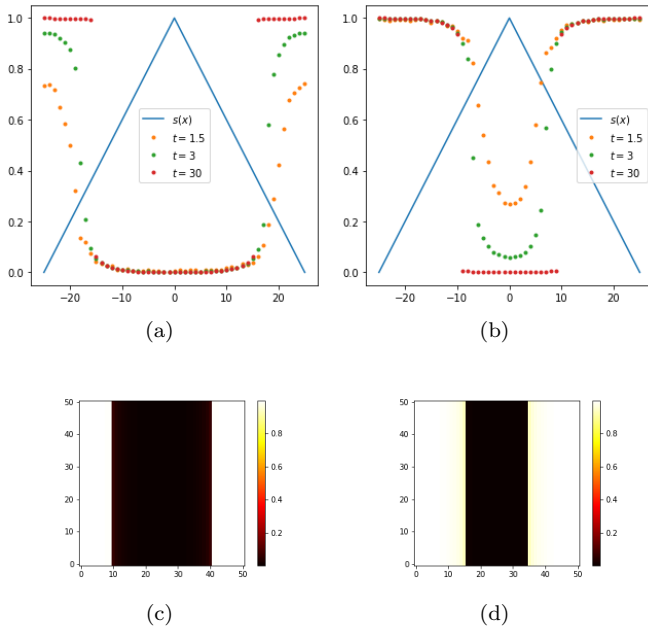


FIG. 2: The blue line corresponds to the profile of the gradient along the x axis and the points corresponds, for different instants, the states adopted for a linear array of cells. Figures (a) and (c) corresponds to the initial condition **A** and (b) and (d) to **B**.

correspondences with the pattern shown.

We studied the dynamics for two initial conditions, all cells at: **A** the epidermal fate $u = 0$ and **B** the SOP fate $u = 1$, with a uniformly distributed random perturbation of the order 10^{-3} .

We can anticipate the result of the pattern by looking at the bifurcation diagram (Fig.1). When the signal is strong (low) enough, cells directly adopt the epidermal (SOP) fate and, it is at intermediate signals that there is bistability. The final states of cells that have an intermediate signal will be regulated by the initial conditions. Each cell will converge to the fate that is more accessible.

This expectation is confirmed numerically (Fig. 2), comparing (Fig. 2a) and (Fig. 2b) we show how the initial conditions influence the dynamics and, comparing (Fig. 2c) and (Fig. 2d) we see that the unique difference between the stationary patterns is the states adopted for those cells under an intermediate signal.

B. Self-organized pattern.

1. Linear stability analysis.

Now the signal each cell receives is the contribution of cells states neighbors (case (ii)). To find the homogeneous state we need to impose $\frac{du_i}{dt} = 0$ and $u_i = u_0, \forall i$.

This gives an implicit equation for u_0 that can be solved numerically using the NR algorithm.

$$u_0 = \frac{1 - \tanh(12u_0)}{2} = 0.09427 \quad (7)$$

As we want to explore the growth of small perturbations around the homogeneous stationary state to evaluate its stability, we took $u_i = u_0 + w_i$ with w_i small. Now the linearized dynamics have the form:

$$\frac{du_i}{dt} = \frac{dw_i}{dt} = (A - 1)w_i - A \sum_{j \in nn_i} w_j \quad (8)$$

with

$$A = \left. \frac{\partial f}{\partial u_i} \right|_{u_0} \quad (9)$$

We can write the equation 8 with matrix notation. This matrix corresponds to the Jacobian of the dynamical system, at the diagonal will contain the terms $(A - 1)$, corresponding to the derivative of $\left. \frac{\partial f}{\partial u_i} \right|_{u_0}$, and at the positions of its neighbors, at the matrix, the term $(-A)$, corresponding to the derivative $\left. \frac{\partial f}{\partial u_j} \right|_{u_0}$.

This corresponds to an $N \times M$ coupled system of equations where N and M are the number of cells along the axis x and y of the lattice. We can solve the entire set of equations by diagonalizing the matrix or reducing the coupling of equation 8 performing the following change of variables:

$$w_i \equiv w_{j,k} = \sum_{q=1}^N \sum_{p=1}^M \eta_{q,p} e^{2\pi i \left(\frac{qj}{N} + \frac{pk}{M} \right)} \quad (10)$$

and the inverse transform:

$$\eta_{q,p} = \frac{1}{MN} \sum_{k=1}^M \sum_{j=1}^N w_{j,k} e^{-2\pi i \left(\frac{qj}{N} + \frac{pk}{M} \right)} \quad (11)$$

Before changing the variables, each cell was mapped to an integer, $i \in 1, 2, \dots, N \times M$. Now cells are represented with two indices j, k referred to the spatial position on the lattice. Introducing this change, we reach to an ordinary system of differential equations, and for each cell the dynamics of the amplitude of the perturbation will be:

$$\frac{d\eta_{q,p}}{dt} = [(A - 1) - A\Omega_{q,p}]\eta_{q,p} = \lambda\eta_{q,p} \quad (12)$$

with

$$\Omega_{q,p} = 2 \left[\cos\left(2\pi \frac{q}{N}\right) + \cos\left(2\pi \frac{p}{M}\right) \right] \quad (13)$$

This function expresses the coupling of equations and is related with the geometry of the lattice. As we said previously the positive real part of eigenvalues correspond to unstable states and negative real part

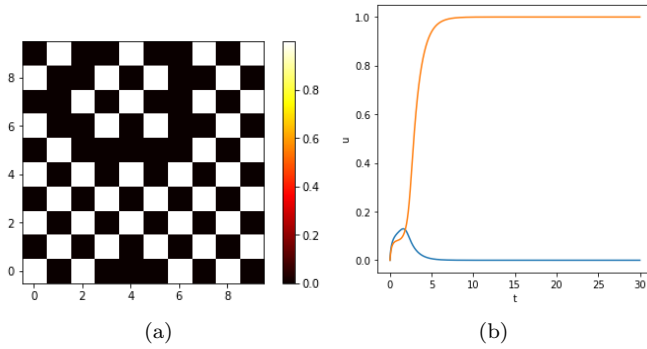


FIG. 3: (a) Pattern formed with cell-cell communication. (b) Evolution of the state u , of two adjacent cell.

to stable states. Thus $Re(\lambda)$ will have to full-fill the following conditions:

$$\begin{array}{ll} \text{Stable:} & \text{Unstable:} \\ A(1 - \Omega_{q,p}) < 1 & A(1 - \Omega_{q,p}) > 1 \end{array} \quad (14)$$

The maximum unstable eigenvalue is the fastest growing mode and it is obtained when $\bar{q} = q/N = 1/2$ and $\bar{p} = p/M = 1/2$. Hence the pattern that emerges from the homogeneous linearly unstable state can be expected to be related with the characteristic period of the modes (\bar{q}, \bar{p}) [11]. So a period 2 along the main directions of the lattice.

2. Numerical integration of the dynamics.

Using the same algorithm of the previous section, with the same values we integrated the dynamics starting with a rather uniform lattice of cell states. We did not have an extracellular signal, so cells were not forced to adopt a particular fate. Now we observed the same two fates as in Fig. 2 but distributed different, creating a fine-grained pattern, typical for lateral inhibition (Fig. 3). This pattern exhibits a period 2 as expect from the linear stability analysis but was not perfect, showing closed contours of low preneuronal activity (epidermal fate).

Although we used the two initial conditions **A** and **B** described before, now we did not observed any difference between the patterns obtained.

The cells that build the contour were not always the same and this contours had a wide range of dimensions. That made us think that one of the mechanisms that could be related with the formation of this contours was the initial conditions. We had a random parameter, the initial perturbation on the cell state. The pattern begins to form at places where the differences between

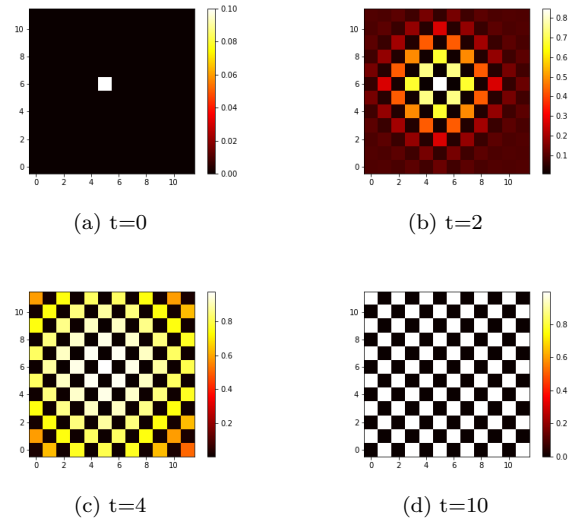


FIG. 4: Evolution of a tissue of 12x12 cells, reaching, at the stationary state, the perfect lateral inhibition pattern.

cells and neighbors states are larger. As the dynamics evolve the pattern expands and the contours are formed when this different patterns, that began at different locations, collapse.

Then if we could begin the formation of the pattern only at one place we would expect the perfect periodic pattern of lateral inhibition. That can be done i.e. by making only at one place a large difference between the cell and its neighbors. This is shown at Fig. 4, where all cells were initially at the same state u and just one cell was different at the center (Fig. 4a). As time progresses the pattern spreads from the center and when all cells reach the stationary state, the perfect periodic pattern is established.

C. Pattern formation in presence of a morphogen gradient and cell-cell interactions.

In this section we studied the formation of a pattern in a tissue of cells having both types of spatial communication. Cells can interact binding the ligand to the receptor of its nearest neighbors, and receive an extracellular signal from the morphogen gradient. So now, the signal is:

$$s = c_i + \sum_{j \in nn} u_j \quad (15)$$

Integrating the dynamics, the system reaches a stable pattern (Fig. 5) that is a superposition of the first two, (Fig 2.) and (Fig 3.), but now cells do not show any

bistable response that depends on the initial condition, in contrast to what we have seen at (Fig. 2). If we begin with the two different initial conditions **A** or **B**, the pattern at the stationary state has the same form (Fig. 5). As the linear analysis as a first approximation

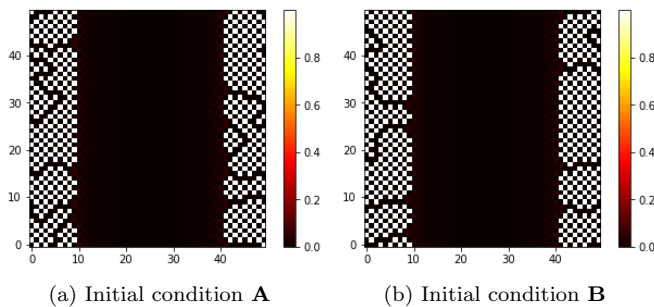


FIG. 5: Evolution of a tissue of 50x50 cells, reaching the same pattern although the dynamics have begun with different initial conditions. The differences between the zones with low extracellular signal it is due to the random perturbation.

is analogous of the last section, but now adding the constant term referred to the morphogen gradient, we did not show here. The homogeneous state is linearly unstable only at the region of low extracellular signal, the rest of cells are rapidly directed to the SOP fate by the high extracellular signal.

IV. CONCLUSIONS

In summary, we showed how cells can differentiate and create spatial patterns using different types of cell communication. The functionality of $f(u, s)$ lets cells choose only between two different fates, having a bistability zone. This was verified dynamically with a

morphogen gradient. In addition, the states that formed the pattern, when there is cell-cell-communication were in correspondence with the curve of the bifurcation diagram and we did not get any state filling in the dotted line since these steady states were unstable.

The morphogen gradient is a plausible mechanism to give positional information to cells and how they have to behave, depending on this extracellular signal. We only investigated the simplest functionality. More sophisticated gradients could drive some different transitions between the two fates [8].

When cells self-organize, using cell-cell interactions, we have shown that the pattern emerges first at places where the differences with its neighbors are larger. Then cells inhibit the adjacent ones to become the same fate reaching the lateral inhibition pattern with a period 2. The imperfections appear when some noise is introduced to the cell state. This could be a subject to further study, may be introducing some correlations between the perturbation of different cells, could let us know how the emerging patterns will collapse. Additionally if a prepattern is established it makes easy to guide fate-specification.

Finally if cells are able to use both types of cell communication, when one predominates heavily onto the other, the pattern arising corresponds to the dominant one. It is worth mentioning that all programs used to compute the calculations and patterns have been build from scratch.

Acknowledgments

I would like to express my gratitude to my advisor Marta Ibañes for accepting me as a TFG student and for many useful discussions.

-
- [1] Koch A. J. and Meinhardt H., *Biological pattern formation: from basic mechanisms to complex structures*, Rev. Mod. Phys. **66**: 1481 (1994)
 - [2] Gilbert SF, *Developmental Biology*, (Sunderland, MA: Sinauer Associates, 2006).
 - [3] Morelli, L. G. et al., *Computational approaches to developmental patterning*, Science, **336**: 6078 187-91 (2012)
 - [4] Gurdon J. and Bourillot PY, *Morphogen gradient interpretation*. Nature **413**: 6858 797-803 (2001).
 - [5] O Shaya, D Sprinzak, *From Notch signaling to fine-grained patterning: Modeling meets experiments*, Current Opinion in Genetics & Development, **21**: 6 732-739 (2011)
 - [6] Barbara H. Jennings, *Drosophila a versatile model in biology & medicine*, Materials Today, **14**: 5 190-195 (2011)
 - [7] Johannes Jaeger, Manu, John Reinitz, *Drosophila blastoderm patterning*, Current Opinion in Genetics & Development, **22**: 6 533-541 (2012)
 - [8] Francis Corson, Lydie Couturier, Herv Rouault, Khalil Mazouni, Francois Schweisguth, *Selforganized Notch dynamics generate stereotyped sensory organ patterns in Drosophila*. Science, American Association for the Advancement of Science, **356**: 6337 (2017)
 - [9] Marc A.T. Muskavitch, *Delta-Notch Signaling and Drosophila Cell Fate Choice*, Developmental Biology, **166**: 2 415-30 (1994)
 - [10] William H. Press, Saul A. Teukolsky, William T. Vetterling, and Brian P. Flannery., *Numerical Recipes 3rd Edition: The Art of Scientific Computing*, (3 ed. Cambridge University Press, New York, NY, USA. 2007)
 - [11] Cross M. C. and Hohenberg P. C., *Pattern formation outside of equilibrium*, Rev. Mod. Phys. **65**: 3 851-1112 (1993)